Electronic Supplementary Material (ESI) for RSC Advances.


Supporting Information

# Engaging Zinc Oxide to Photo-Transform Aromatic and Aliphatic alcohols with a Photo-Physical Interpretation at the Alizarin Red-Zinc Oxide Interface.

**Timothy M. Underwood[a] and Ross S. Robinson.[a*]**

[a.] School of Chemistry and Physics, University of KwaZulu-Natal, Scottsville, Pietermaritzburg, 3209, South Africa. e-mail: robinsonr@ukzn.ac.za

Table of Contents

## S1. Instrumentation

Mass spectrometry data was recorded on a Shimadzu QP2010 SE gas chromatograph-mass spectrometer with the following conditions: Gas chromatograph: oven temperature (120 ˚C), injection temperature (250 ˚C) and injection mode (split). Column specifications: InterCap 5MS/Sil, Thickness: 0.25 μm, diameter: 0.25 mm and length: 30.00 meters. Mass Spectrometer: Ion Source temperature: 200 ˚C, interface temperature: 200 ˚C and solvent cut time: 1.9 minutes. Photoluminescence data was recorded on a Horiba iHR320 monochromator with signal detection being obtained from a photomultiplier connected to a lock on amplifier. Light emissions were recorded from 360 to 900 nm with an excitation wavelength of 325 nm from a continuous He-Cd laser (laser pulse limited to 120 Hz). Sample collection was recorded in triplicate and averaged to produce the presented results. The samples were mounted as thin powdered films. The irradiation source was an OSRAM VIALOX bulb connected to a Tridonic transformer (80 W, 0.8 A, 230 V, 50 Hz). Powdered semiconductor samples were studied on a Shimadzu UV-2600 UV/Vis spectrophotometer that was equipped with a Shimadzu ISR-2600/ISR-2600 Plus integrating sphere attachment.

## S2. Preparation of dye sensitised zinc oxide powder

Drop wise addition of de-ionised water (*ca.* 200 uL) to a powdered mixture of Alizarin Red S organic dye (BDH Indicators, C.I. 58005, 0.025 g, 0.073 mmol) and zinc oxide (Zinc oxide: Hugh Source (International) LTD, 99.5 % minimum, 0.975 g, 12.00 mmol) afforded a consistent thick purple paste that was stirrer over night until dry. The dried powder was crushed in a pestle and mortar to form alizarin red sensitized zinc oxide photocatalytic powder (purple in colour).

### S2.1. Estimation of adsorbed alizarin red S on the surface of ZnO using powder diffuse reflectance spectroscopy and infrared spectroscopy.

There have been limited literature discussions on quantifying the degree of chemically adsorbed dyes onto the surface of metal oxides. However, Yoon *et al.*[1] utilized a UV/Vis spectroscopic technique to estimate the quantity of an adsorbed ethanolic solution of N719 cis-bis(isothiocyanato)bis(2,2’-bipyridyl-4,4’-dicar-boxylato) ruthenium(II)bistetrabutylammonium Ru[II] organic complex on titanium dioxide after

desorbing the dye using a sodium hydroxide solution and comparing the absorption spectrum again referenced concentrations. In the undertaken research, all of the alizarin red S (0.025g) was magnetically stirred with zinc oxide (0.975g) using minimal water until dryness. Therefore, to estimate the quantity of adsorbed alizarin red S on ZnO, a solid state infrared titration of different weight percentages (wt.%) alizarin red S on ZnO were prepared to monitor the intramolecular hydrogen bonding (-OH) stretching frequency between the hydroxy group (**Figure 1**, position 16 ) of the catecholate moiety and the adjacent carbonyl group of alizarin red (**Figure 1**, position 15). Upon the re-appearance of the intramolecular hydrogen bonding (-OH) stretching frequency at higher wt.% of alizarin red (up to 35 wt.%), an estimation of the quantity of alizarin red that was chemically bound to ZnO could be obtained.

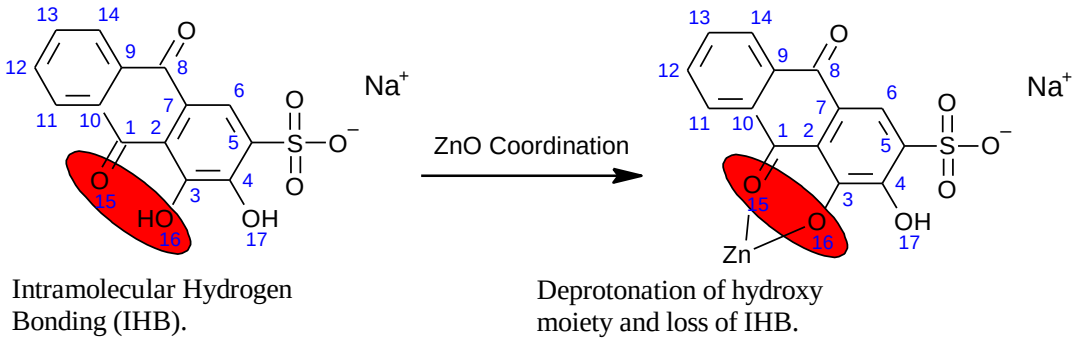


Intramolecular Hydrogen Bonding (IHB).

Deprotonation of hydroxy moiety and loss of IHB.

**Figure 1:** Predicted coordination of alizarin red S to ZnO with loss of intramolecular hydrogen bonding (IHB).

The solid state infrared titration was performed using an alizarin red wt.% range (0.1 to 35 wt.%) on ZnO to monitor the intramolecular hydrogen bonding (-OH) stretching frequency upon coordination of alizarin red S to ZnO (**Figure 2**).

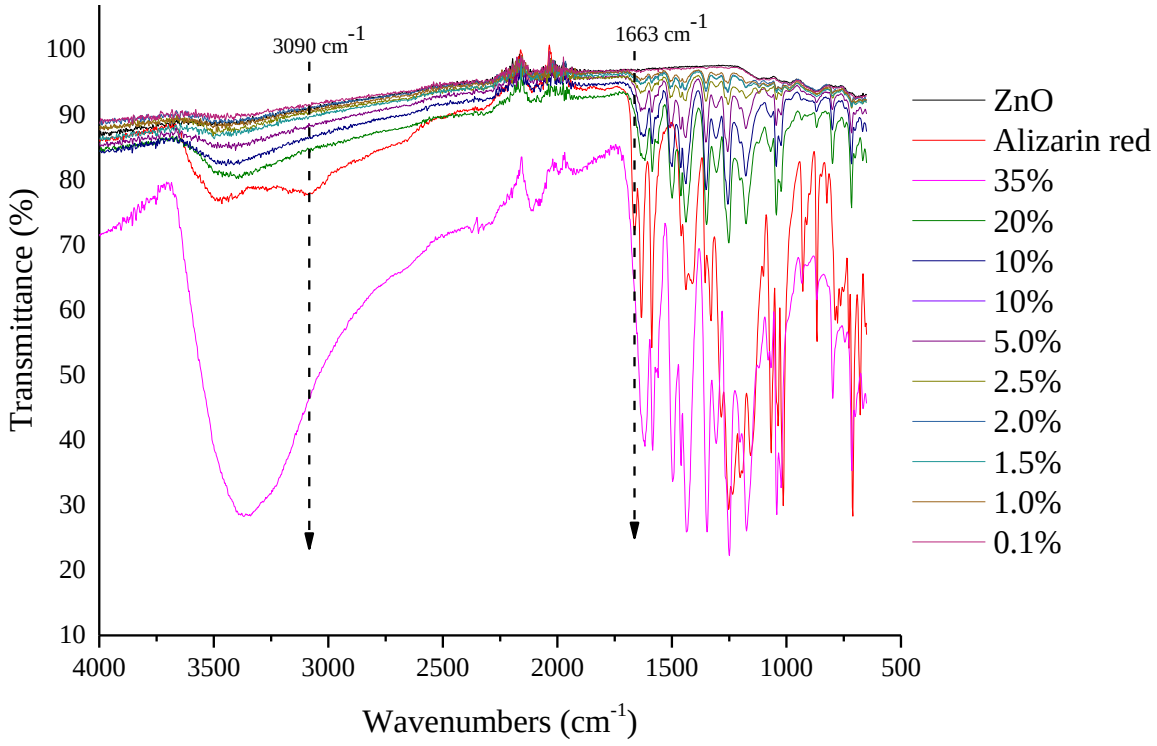


**Figure 2:** Solid state infrared titration of alizarin red S (0.1 to 35 wt.%) on ZnO. The spectra have demonstrated how the loss of the broad shoulder at 3090 $cm^{-1}$ are indicative of alizarin red S losing the intramolecular hydrogen bonding (-OH) stretching frequency between the hydroxy and adjacent carbonyl moieties (**Figure 1**, positions 16 and 15, respectively) upon coordination to ZnO. An expanded view of the Fingerprint region has been graphically represented in **Figure 3**.

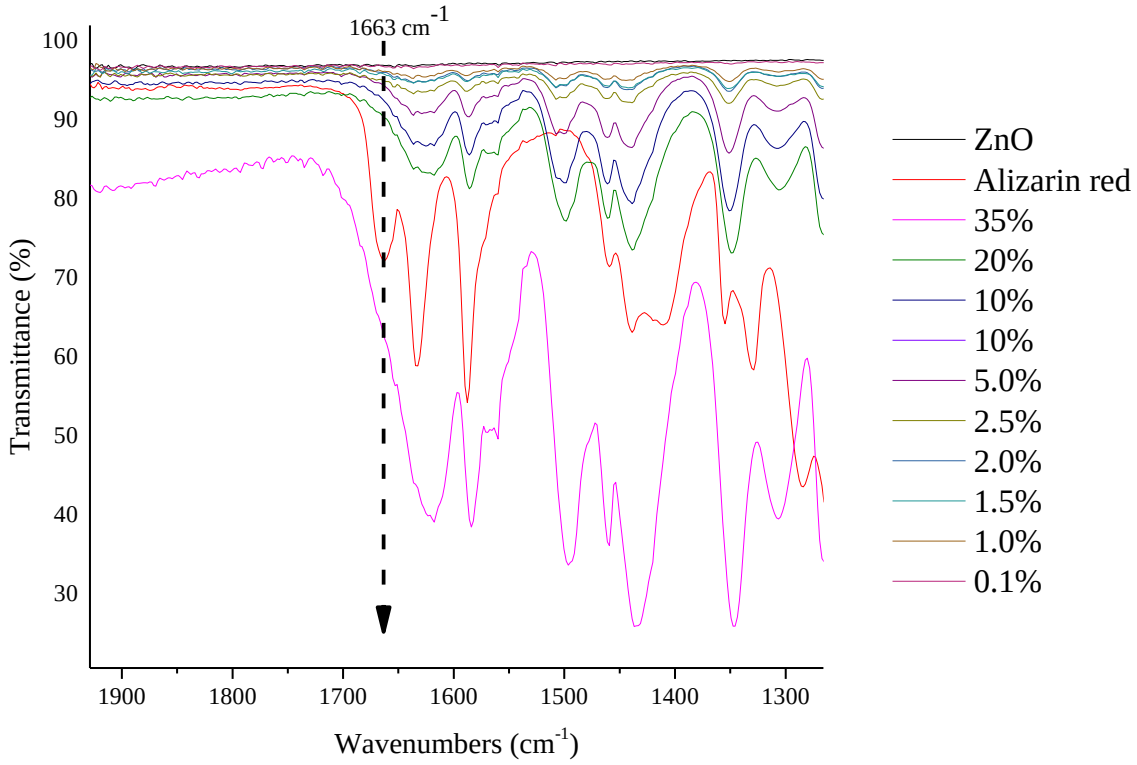


**Figure 3:** Expanded Fingerprint region of alizarin red sensitised ZnO. A noticeable absence of the carbonyl stretching frequency at 1663 $cm^{-1}$ in all alizarin red sensitised ZnO samples (0.1 to 35 wt.%) indicated the coordination of all the alizarin red to zinc oxide.

As reported in **Figure 2**, the intramolecular hydrogen bonding (-OH) stretching frequency at 3090 $cm^{-1}$ (**Figure 1**, position 16) for alizarin red S (solid red line, which is in agreement with the literature[2]) was absent for all alizarin red sensitised zinc oxide samples (0.1 to 20 wt.%). When the wt.% loading of alizarin red was increased to 35 wt.%, the absence of the 3090 $cm^{-1}$ further substantiated that all the alizarin red S had effectively chemically adsorbed onto the surface of zinc oxide. **Figure 3** has further demonstrated that the absence of any carbonyl stretching frequency (1663 $cm^{-1}$) in any of the alizarin red sensitised ZnO samples (0.1 to 35 wt.%) lent additional evidence to motivate complete coordination of alizarin red to ZnO up to wt.% loadings of 35%.

The alizarin red sensitised zinc oxide samples (0.1 to 2.5 wt.% alizarin red loadings) were also studied using powder diffuse reflectance spectroscopy in both reflectance and absorbance modes (**Figure 4**).

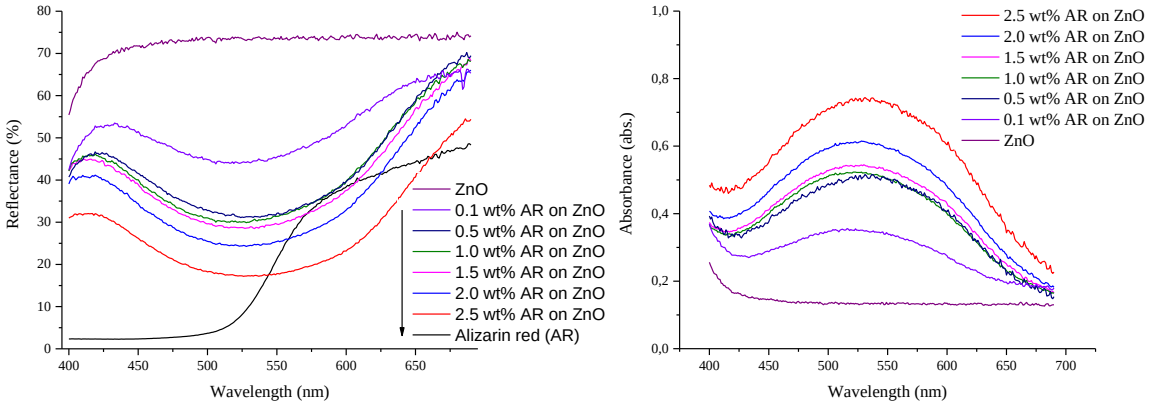


**Figure 4:** Powder UV/Vis spectroscopy spectra of alizarin red sensitised ZnO (0.1 to 2.5 wt.% alizarin red). The spectra of reflectance data (left) and absorbance data (right) both demonstrate identical reflectance and absorbance profiles, respectively, and therefore a consistent chemical adsorption between alizarin red and zinc oxide over a range of alizarin red wt.% loadings (0.1 to 2.5 wt.%).

A graphical experiment was further conducted to illustrate that alizarin red sensitised zinc oxide was stabilised in water with an ionic salt solution of silver nitrate and sodium nitrate (1.24 M). It has been previously reported in the literature that silver solutions are known to stabilise dye sensitised photocatalytic systems, while in other reports, anthocyanin extracts have been noticeably stabilised in the presence of Mg, Fe, K, Cu, Al and Sn ions due to the presence of hydroxy groups that co-ordinate and stabilise the organic dye.[3],[4] Due to the solubility of alizarin red S (1 mg/mL) in water,[5] the ionic salt stabilising effect of the silver-sodium nitrate was assessed. Aqueous mixtures (**Figure 5**) of alizarin red sensitised zinc oxide with and without $AgNO_3$ and $NaNO_3$ (1.24 M) were prepared.

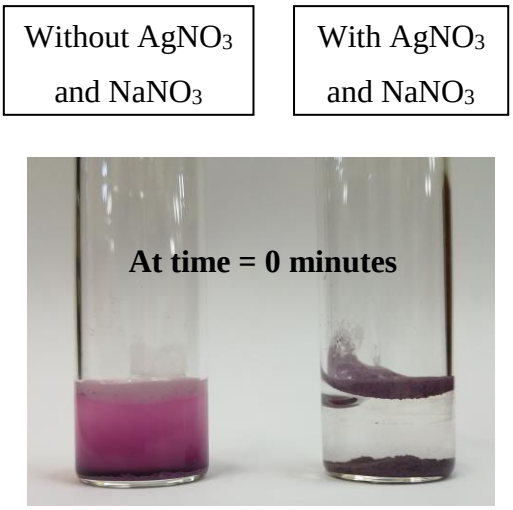


**Figure 5:** Graphical representation of alizarin red sensitised zinc oxide in water with and without $AgNO_3$ and $NaNO_3$ at t = 0. Without the presence of the Ag-Na ionic stabilising solution, alizarin red was seen to significantly desorbed from the zinc oxide surface upon preparation.

## S3. General experimental procedure to synthesis 4-nitrobenzaldehyde.

To a 5 ml quartz glass test tube, d-ZnO (20 mg) was added to a prepared silver nitrate ($AgNO_3$ [1 equivalent, 34 mg] and $NaNO_3$ [3 equivalents, 51 mg] in 0.5 ml de-ionised water) solution that was left to stir for three minutes to produce a homogeneous silver-sodium solution. 2,2,6,6-tetramethylpiperidine-N-oxyl (TEMPO, 9.6 x $10^{-5}$ mol) and 3-dimethybenzyl alcohol (0.2 mmol,) were subsequently added to the silver nitrate/sodium nitrate aqueous solution. The test tube was positioned five centimeters in front of an incandescent radiation source (hv > 450 nm) for a period of seven hours. After the completion of the reaction, the contents were extracted into 3 x 1 mL dichloromethane. The crude product (*ca.* 80 ppm solution) was prepared for quantitative analysis on a Shimadzu QP 2010SE gas chromatograph-mass spectrometer.

## S4. Quantitative formulations to detect the remaining alcohol after the reaction process.

The conversion of alcohols into aldehydes was quantitatively measured using gas chromatography-mass spectrometry (GC-MS) on a Shimdazu QP2010SE equipped with a Zebron ZB-5MSplus column. Gas chromatography was the chosen quantitative technique to determine the oxidised product due to the low reaction scale (0.2 mmol).

Therefore, an internal standard (4-octylphenol) was calibrated against each alcohol tested after which, relative response factors were calculated and used as references to determine the amount of unreacted alcohol that remained after each photocatalytic reaction, and hence the alcohol conversion.

The response factor of the selected alcohol was based upon the relationship between peak area and the concentration of the alcohol, as noted in **Equation 1**:

$$RF = \frac{PA_A}{[A]} \qquad \textbf{Equation 1}$$

Where: * RF = Response factor
* $PA_A$ = Peak area of the alcohol
* [A] = Alcohol concentration

Furthermore, in order to establish the association between the alcohol with the internal standard, which would later serve to quantify the remaining alcohol in the reaction test, a response factor of the alcohol relative to the internal standard needed consideration (**Equation 2**).

From the expression,

$$RRF = \frac{RF_A}{RF_{IS}} \qquad \textbf{Equation 2}$$

Where: * RRF = Relative response factor
* $RA_A$ = Response factor of the alcohol
* $RF_{IS}$ = Response factor of the internal standard

Consider for example **Figure 6**:

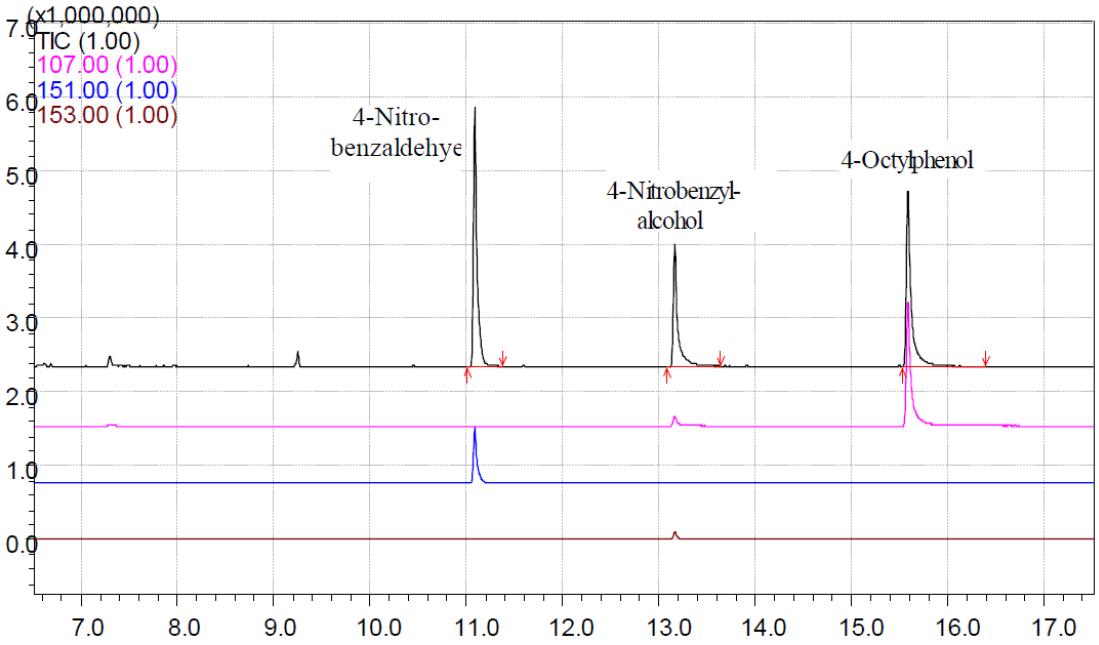


**Figure 6:** The chromatogram representing the oxidation of 4-nitrobenzyl alcohol to 4-nitrobenzaldehyde and the presence of the internal standard (4-octylphenol) to quantitate the reaction progress.

The peak areas of 4-nitrobenzyl alcohol, 4-nitrobenzaldehyde and 4-octylphenol were integrated to obtain their respective values (4-nitrobenzyl alcohol [5272312], 4-nitrobenzaldehyde [8754300] and 4-octylphenol [5361877]) in **Figure 6**.

From an independent response factor chromatogram, the response factor for 4-nitrobenzyl alcohol (131809.09) was calculated. From these response factors, the relative response factor to the internal standard was subsequently determined (4-nitrobenzyl alcohol [0.78]). The relative response factor values of the alcohols used in the photo-oxidation studies have been tabulated below (**Table 1**).

**Table 1:** Relative response factors for the alcohols and aldehydes used in the photo-oxidation studies

| | **Relative Response Factors (RRF)** |
|---|---|
| **Alcohols** | **Alcohol (OH)**<br>**RRF (OH)** |
| 3,4-Dimethoxybenzyl alcohol | 1,11 |

Table continues overleaf

| | |
|---|---|
| 4-Methoxybenzyl alcohol | 1,12 |
| 4-Nitrobenzyl alcohol | 0,78 |
| 2-Naphthalene methanol | 1,62 |
| Cinnamyl alcohol | 1,23 |
| 3-Clorobenzyl alcohol | 0,99 |
| Benzyl alcohol | 1,14 |
| Cyclohexanol | 0,77 |
| 4-Methylbenzyl alcohol | 0,88 |
| Furfuryl alcohol | 0,41 |
| Benzoin | 0,96 |
| 2-Hydroxyphenethyl alcohol | 0,85 |
| 1-Hexanol | 0,51 |
| 1-Heptanol | 0,74 |
| trans-2-Hexen-1-ol | 0,53 |
| 2-Decanol | 0,57 |
| 2,2-Dimethyl-1,3-propanediol | 0,41 |

Once the quantitative parameter was collected (the relative response factor for 4-nitrobenzyl alcohol), the sample (**Figure 6**) could be quantitatively analysed.

The concentration of the remaining 4-nitrobenzyl alcohol after the reaction was calculated from knowing the response factor of 4-nitrobenzyl alcohol and 4-octyl phenol after combining **Equation 1** and **Equation 2**:

$$[A] = PA_A \times \frac{[IS]}{PA_{IS}} \times \frac{1}{RRF_A}$$ **Equation 3**

For example: The oxidation of 4-nitrobenzyl alcohol to 4-nitrobenzaldehyde (**Figure 7**).

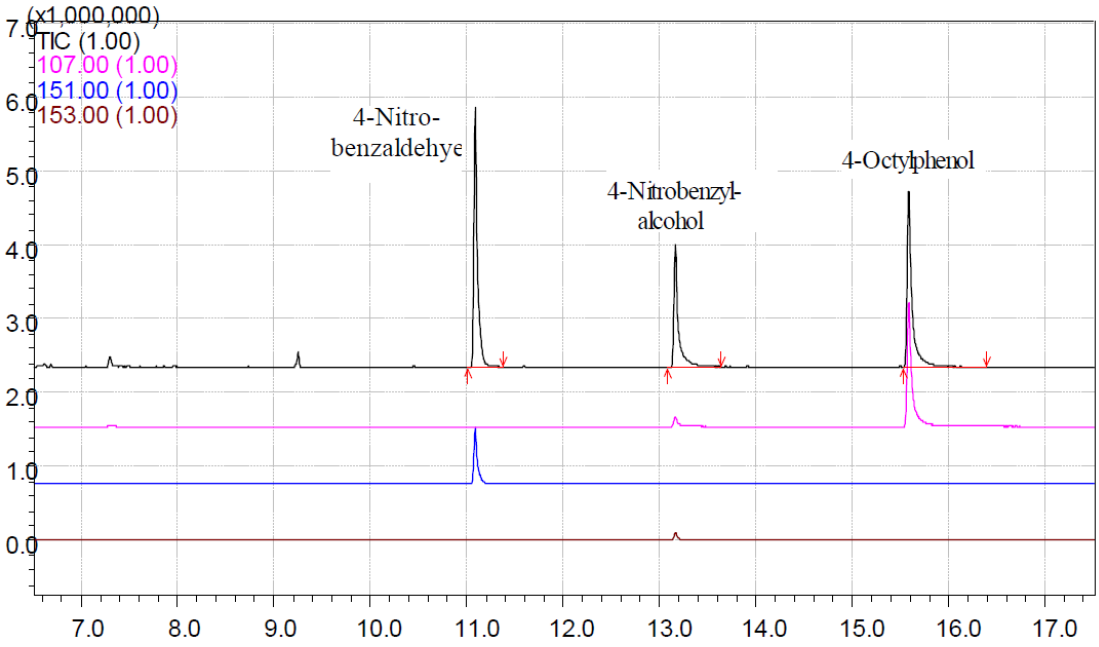


**Figure 7:** The chromatogram representing the oxidation of 4-nitrobenzyl alcohol to 4-nitrobenzaldehyde using Cu/Pd-N-$TiO_2$.

Calculations:

$$[\mathrm{OH}] = \mathrm{PA_{OH}} \times \frac{[\mathrm{IS}]}{\mathrm{PA_{IS}}} \times \frac{1}{\mathrm{RRF_{OH}}}$$

$$= \mathrm{PA_{OH}} \times \frac{[\mathrm{IS}]}{\mathrm{PA_{IS}}} \times \frac{1}{\frac{\mathrm{RF_{OH}}}{\mathrm{RF_{IS}}}}$$

$$= 5272312 \times \frac{31.52}{5361877} \times \frac{1}{\frac{131809.09}{170019.28}}$$

$$= 39.98 \text{ ppm } \pm 6.67\ \%$$

The concentration (39.98 ppm) of 4-nitrobenzyl alcohol noted above was the remaining alcohol in the reaction solution after the seven-hour reaction period.

Note: Prior to analysing the reaction contents (**Equation 3**), the crude mixture was too concentrated for a direct injection into the GC-MS. An approximate analyte concentration of 80 ppm was prepared as it was within the calibration curve's concentration range (20−140 ppm). The sample dilution (to achieve an *ca.* 80 ppm analyte solution) was prepared accordingly:

Sample dilution factor:

Assuming 0 % conversion of 0.1 mmol 4-nitrobenzyl alcohol in 2.5 mL toluene (reaction solvent), the alcohol concentration would be calculated as follows:

mmol of 4-methylbenzyl alcohol = 15.31 mg
15.31 mg in 2.50 mL = 6124.00 ppm

To achieve an alcohol concentration of *ca.* 80 ppm, a 59.38× dilution was introduced (25.26 μL of the reaction analyte in 1474.47 μL of solvent). The total volume prepared for GC-MS analysis = 1.5 mL.

At 0 % conversion, the concentration of 4-nitrobenzyl alcohol was:
= 6124.00/59.38
= 103.13 ppm

The conversion of 4-nitrobenzyl alcohol was then determined as follows:

$$C = \frac{[OH]^0 - [OH]^t}{[OH]^0} \times 100$$

where $[OH]^0$ = alcohol concentration at the start of the reaction, *i.e.* 0% conversion and $[OH]^t$ = alcohol concentration remaining at the end of the reaction period 't'.

$$C = \frac{103.13 - 39.98}{103.13} \times 100$$

= 61 %

## S5. Raw chromatographic data

# Table 2

Entry 1

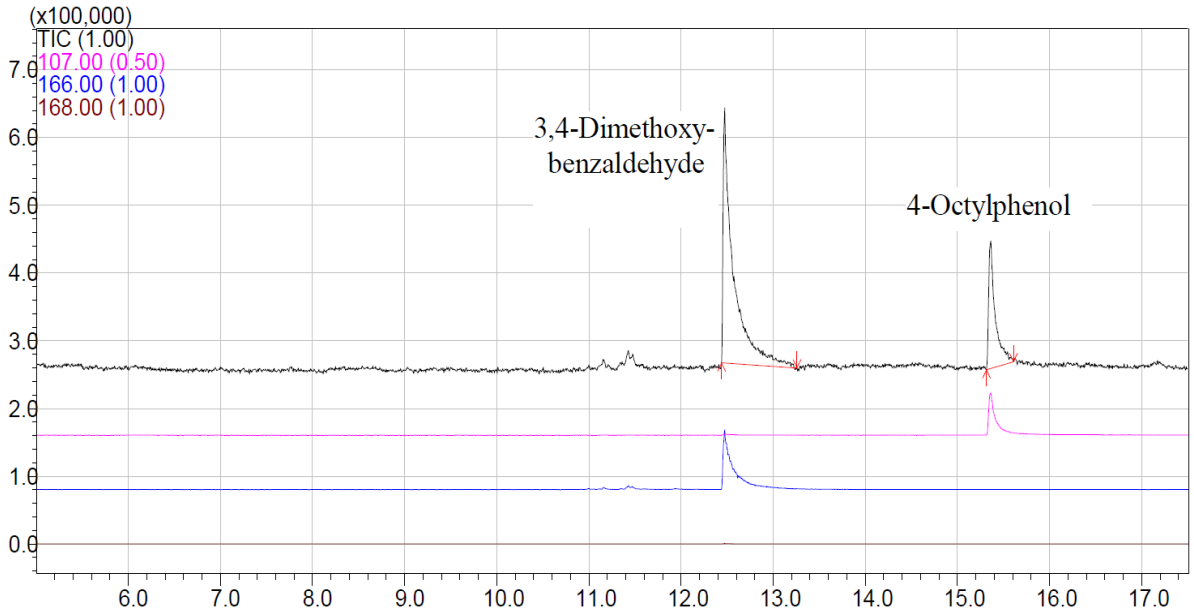


Entry 2

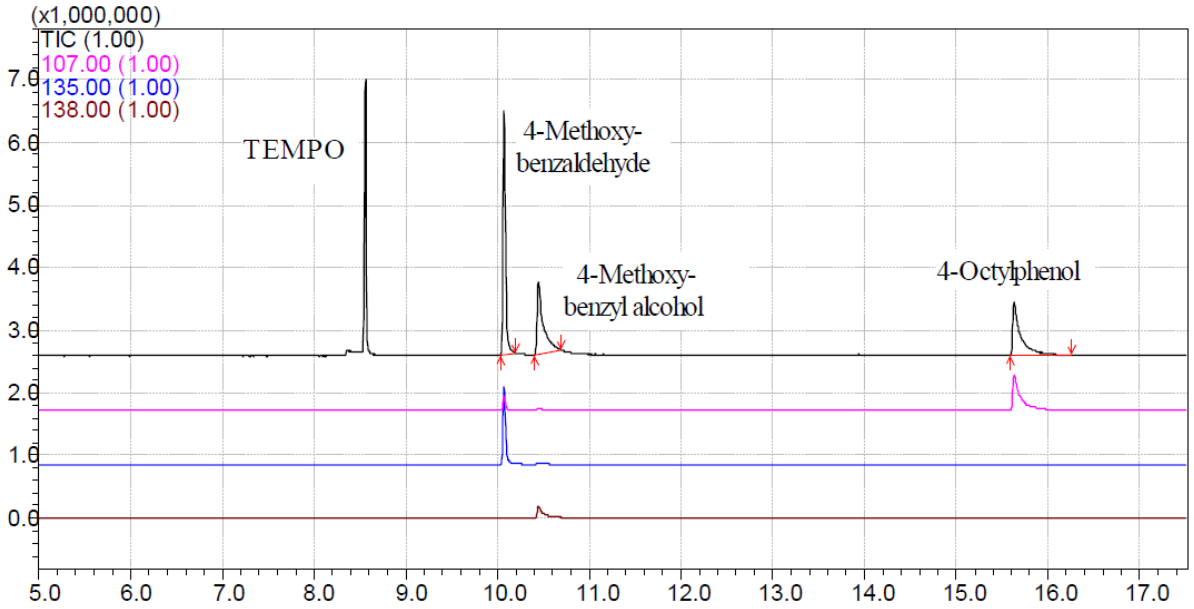

Entry 3

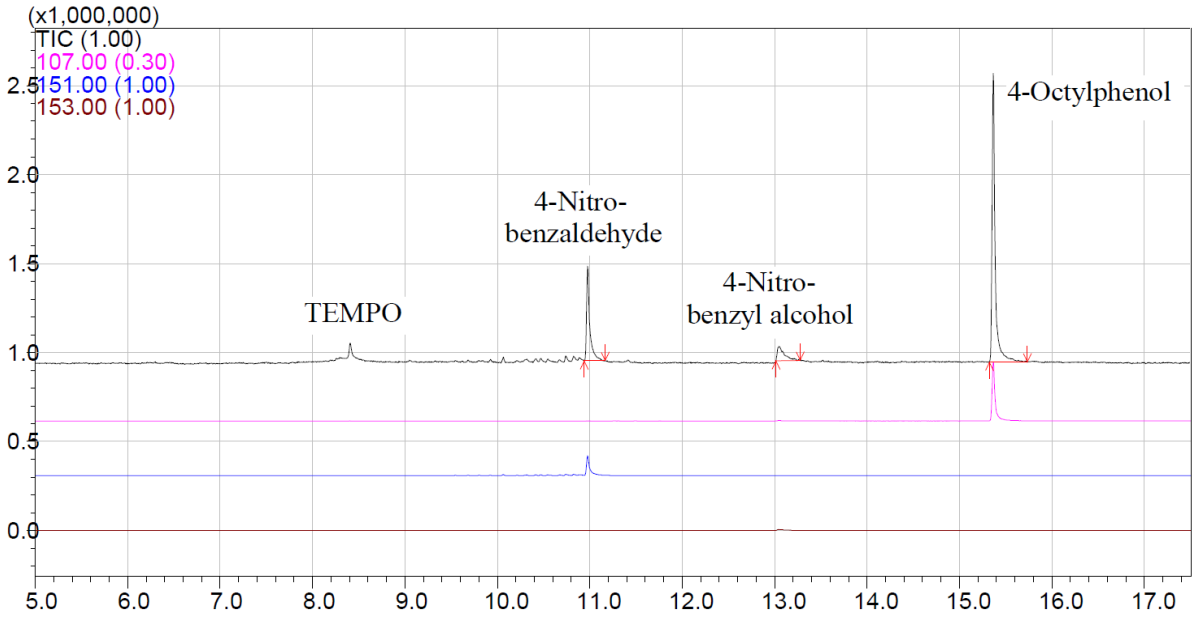


Entry 4

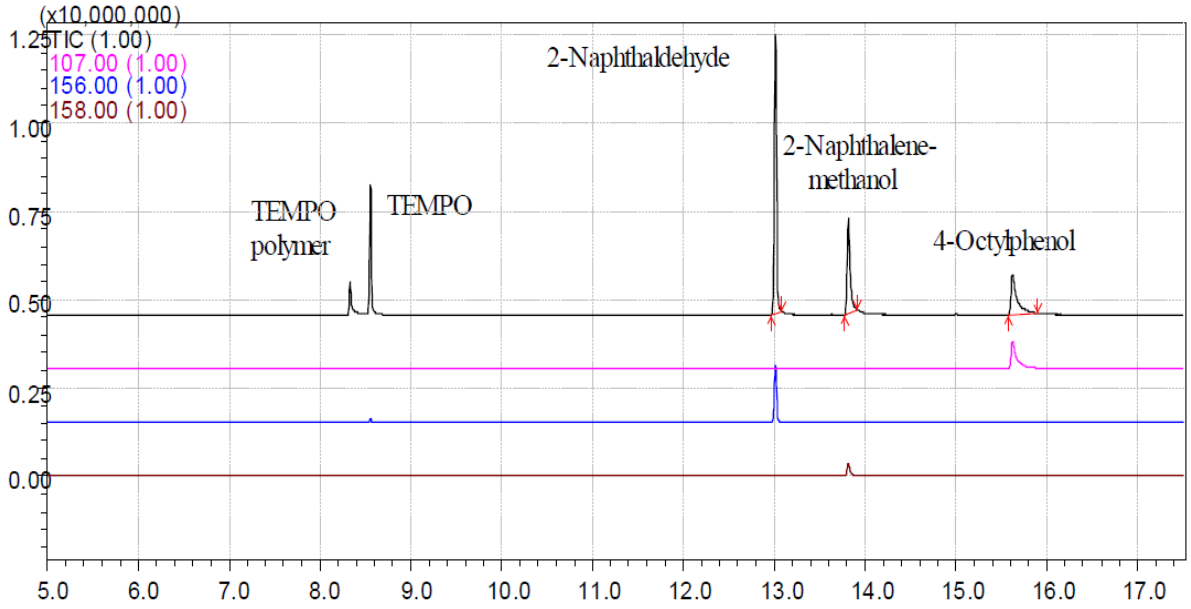

Entry 5

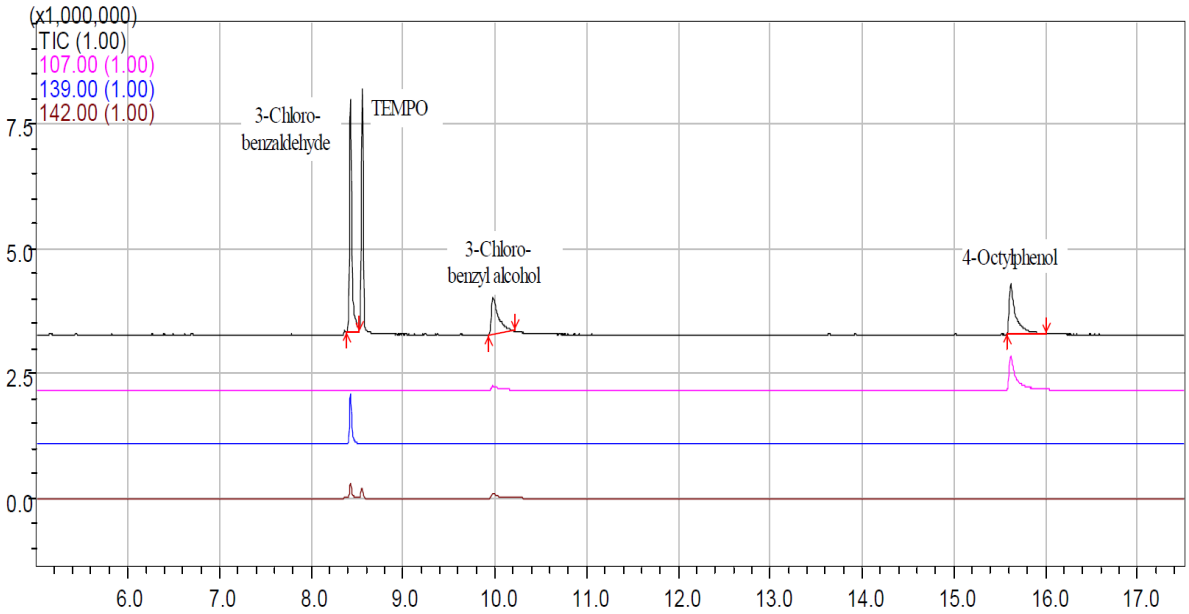


Entry 6

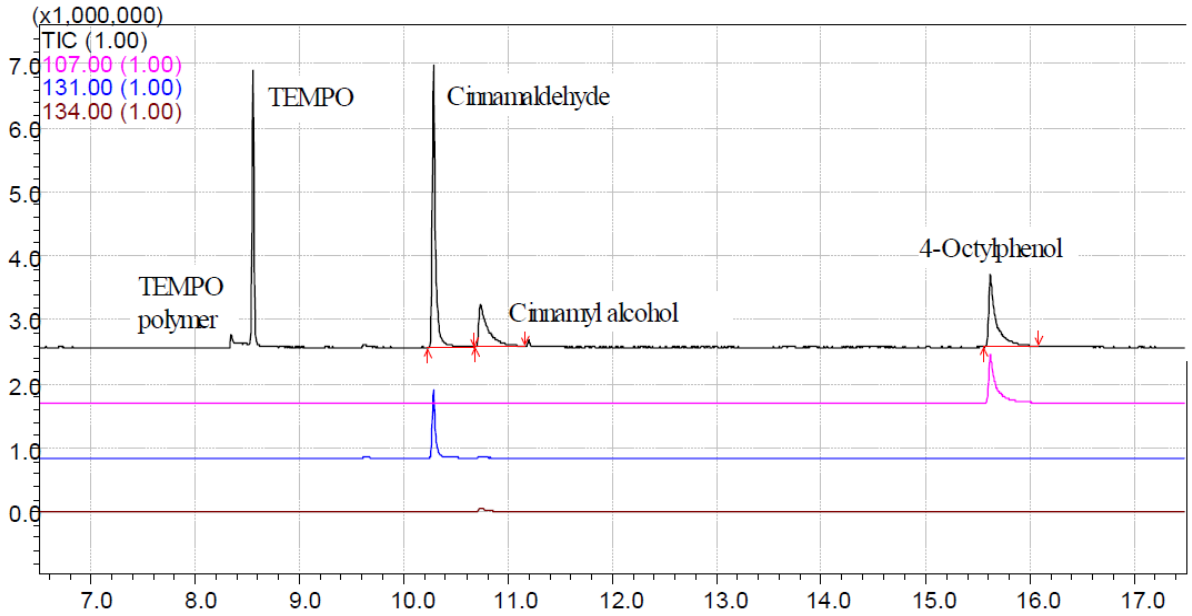

Entry 7

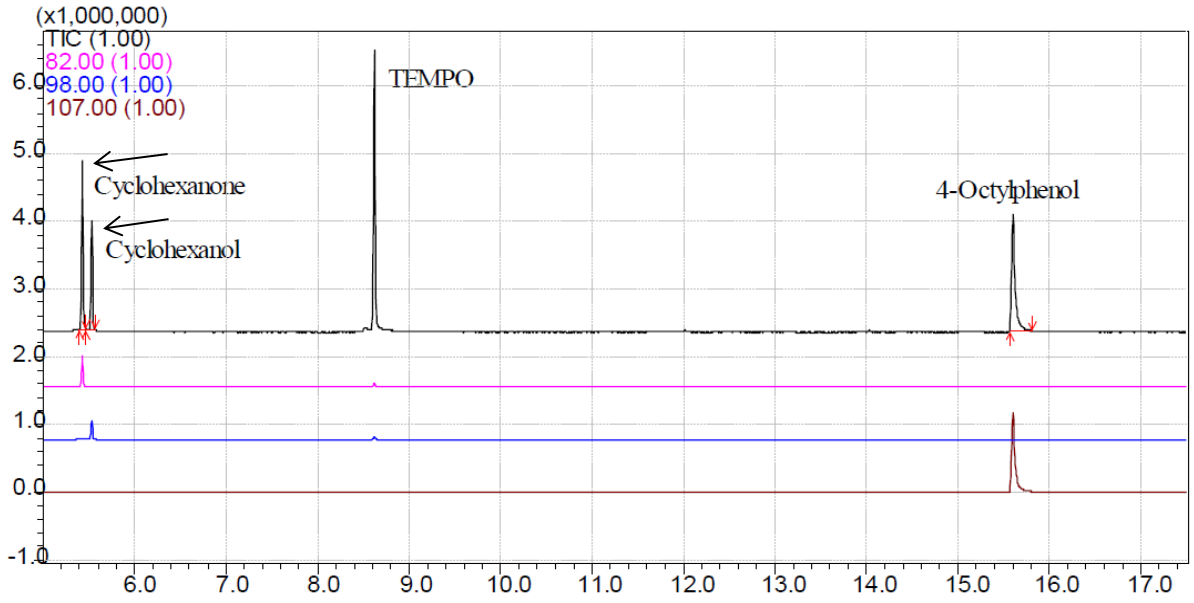


Entry 8

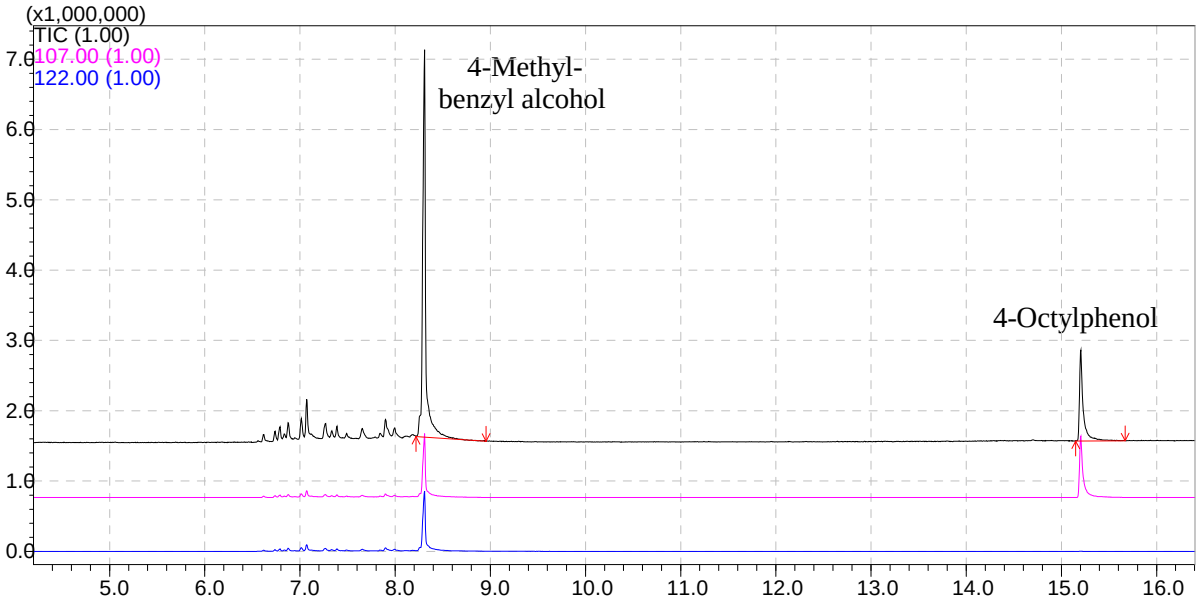

Entry 9

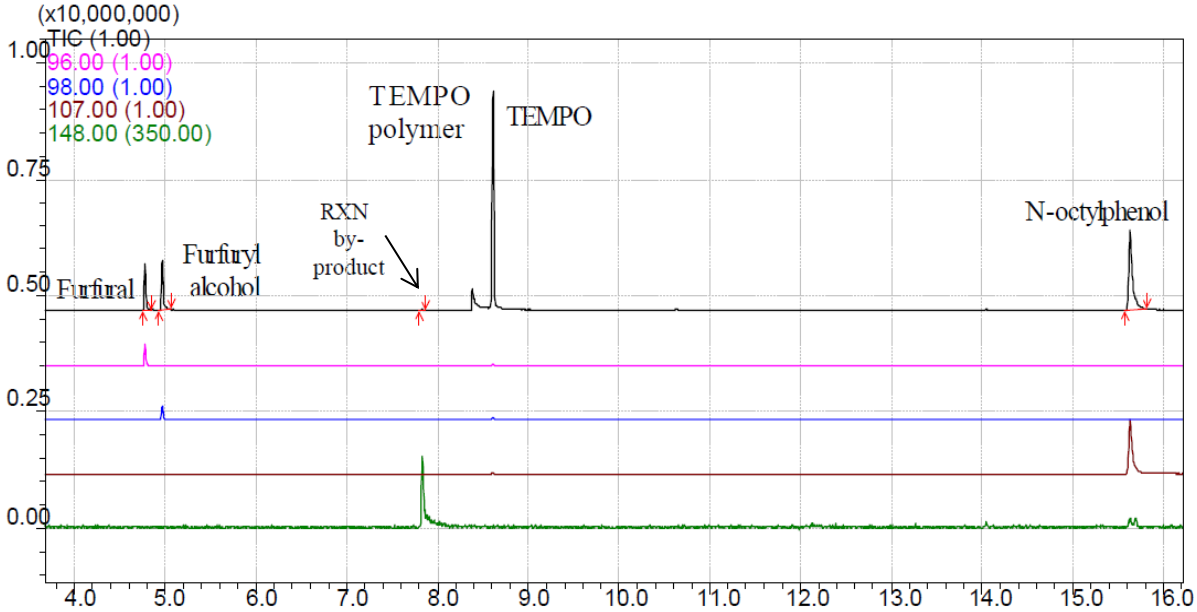


Entry 10

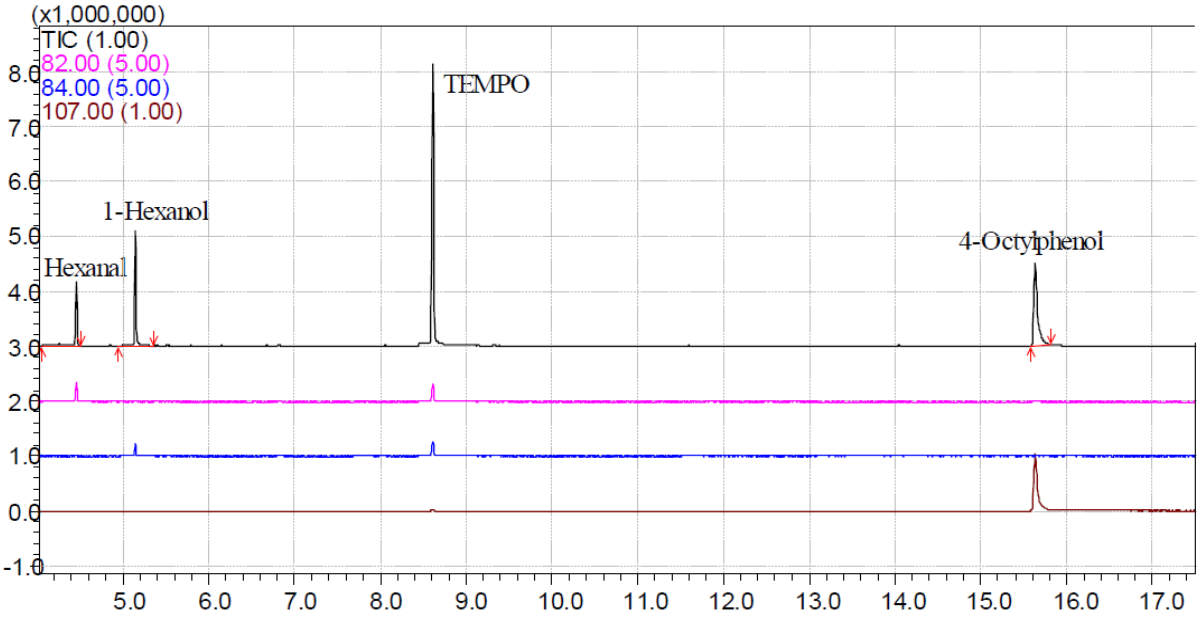

Entry 11

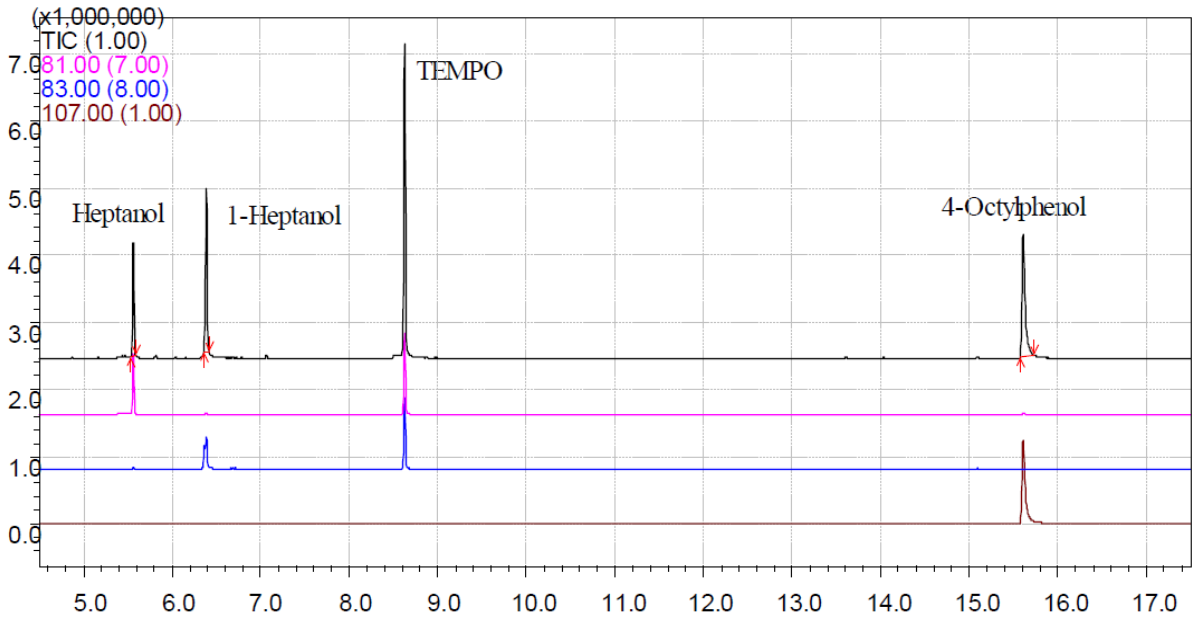


Entry 12

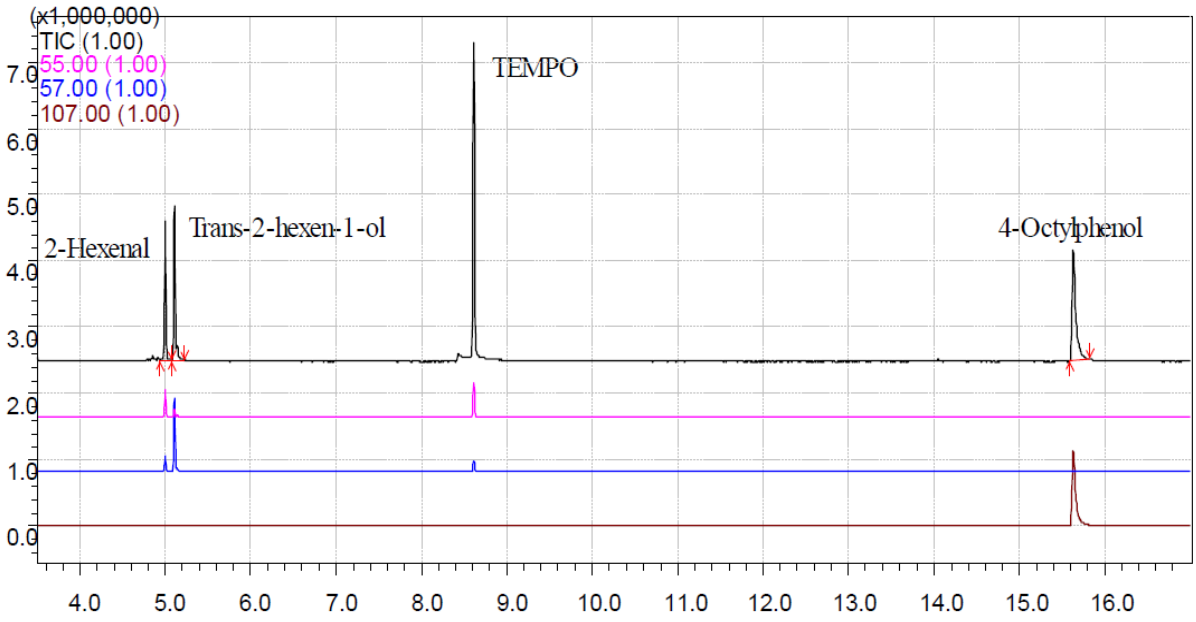

Entry 13

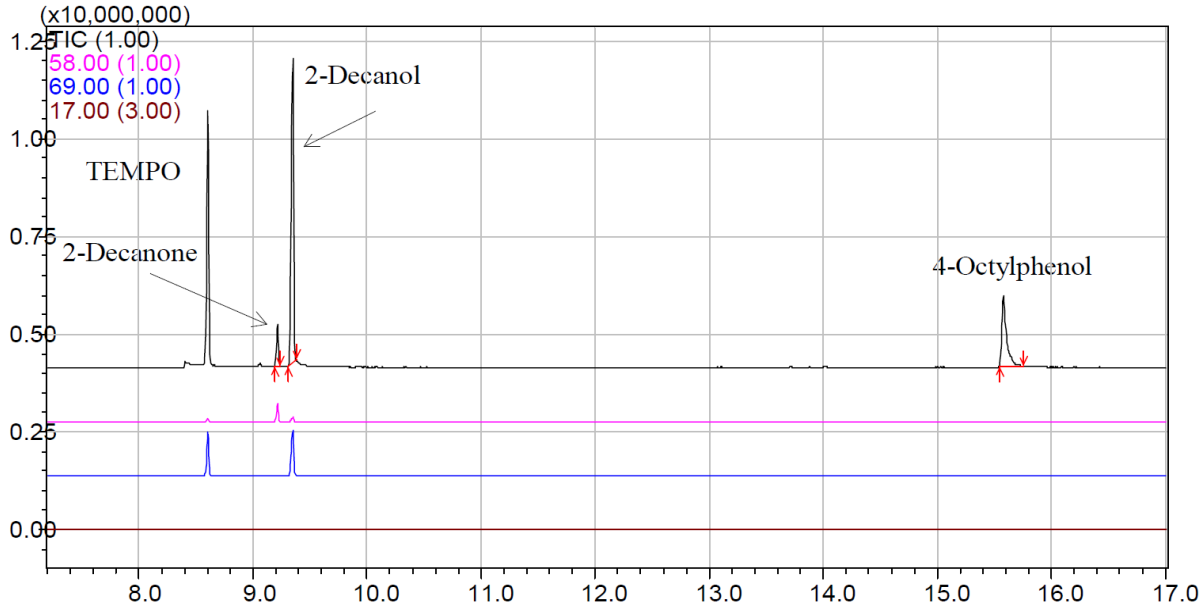


Entry 14

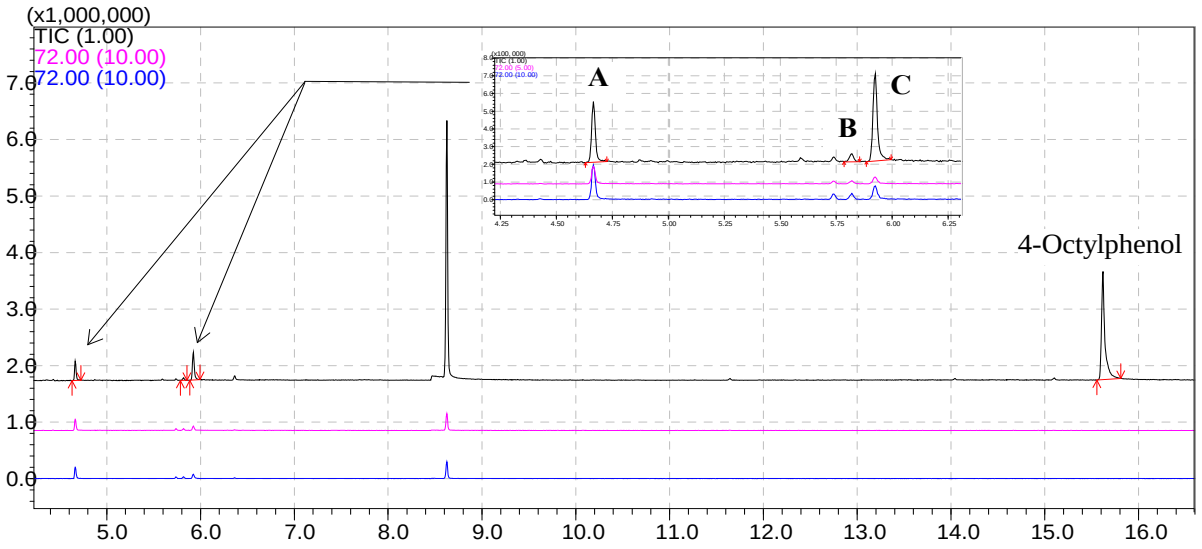


A = 2,2 dimethyl-3-hydroxypropionaldehyde  B = Side product  C = 2,2-dimethyl-1,3-propandiol

## S6. Density Functional Theory Supporting information

References used in the manuscript:


14. Frisch, M. J.; Trucks, G. W.; Schlegel, H. B.; Scuseria, G. E.; Robb, M. A.; Cheeseman, J. R.; Scalmani, G.; Barone, V.; Mennucci, B.; Petersson, G. A.; Nakatsuji, H.; Caricato, M.; Li, X.; Hratchian, H. P.; Izmaylov, A. F.; Bloino, J.; Zheng, G.; Sonnenberg, J. L.; Hada, M.; Ehara, M.; Toyota, K.; Fukuda, R.; Hasegawa, J.; Ishida, M.; Nakajima, T.; Honda, Y.; Kitao, O.; Nakai, H.; Vreven, T.; Montgomery Jr., J. A.; Peralta, J. E.; Ogliaro, F.; Bearpark, M. J.; Heyd, J.; Brothers, E. N.; Kudin, K. N.; Staroverov, V. N.; Kobayashi, R.; Normand, J.; Raghavachari, K.; Rendell, A. P.; Burant, J. C.; Iyengar, S. S.; Tomasi, J.; Cossi, M.; Rega, N.; Millam, N. J.; Klene, M.; Knox, J. E.; Cross, J. B.; Bakken, V.; Adamo, C.; Jaramillo, J.; Gomperts, R.; Stratmann, R. E.; Yazyev, O.; Austin, A. J.; Cammi, R.; Pomelli, C.; Ochterski, J. W.; Martin, R. L.; Morokuma, K.; Zakrzewski, V. G.; Voth, G. A.; Salvador, P.; Dannenberg, J. J.; Dapprich, S.; Daniels, A. D.; Farkas, Ö.; Foresman, J. B.; Ortiz, J. V.; Cioslowski, J.; Fox, D. J. Gaussian 09, Gaussian, Inc.: Wallingford, CT, USA, 2009.
15. Becke, A. D., The Journal of Chemical Physics 1993, 98 (7), 5648-5652.
16. Lee, C.; Yang, W.; Parr, R. G., Physical Review B 1988, 37 (2), 785-789.
17. Vosko, S. H.; Wilk, L.; Nusair, M., Canadian Journal of Physics 1980, 58 (8), 1200-1211.
18. Stephens, P. J.; Devlin, F. J.; Chabalowski, C. F.; Frisch, M. J., The Journal of Physical Chemistry 1994, 98 (45), 11623-11627.
19. McLean, A. D.; Chandler, G. S., The Journal of Chemical Physics 1980, 72 (10), 5639-5648.
20. Krishnan, R.; Binkley, J. S.; Seeger, R.; Pople, J. A., The Journal of Chemical Physics 1980, 72 (1), 650-654.


Supporting Information References:


[1] H.-S. Yoon, X.-H. Ho, J. Jang, H.-J. Lee, S.-J. Kim, H.-Y. Jang, *Organic Letters* **2012**, *14*, 3272-3275.
[2] L. Legan, K. Retko, P. Ropret, *Microchemical Journal* **2016**, *127*, 36-45.
[3] V. Jeena, R. S. Robinson, *Chemical Communications* **2012**, *48*, 299-301.
[4] R. Cortez, D. A. Luna-Vital, D. Margulis, E. Gonzalez de Mejia, **2017**, *16*, 180-198.

[5] S. Aldrich, in *Alizarin Red S* (Ed.: S. Aldrich), The SIGMA-ALDRICH Group.